Polymer 56 (2015) 256–262

Contents lists available at ScienceDirect

Polymer

journal homepage: www.elsevier.com/locate/polymer

Specific features of the environmental crazing of poly(ethylene terephthalate) fibers

O.V. Arzhakova*, A.A. Dolgova, L.M. Yarysheva, A.L. Volynskii, N.F. Bakeev

Faculty of Chemistry, Lomonosov Moscow State University, Leninskie Gory, Moscow 119991, Russia

ARTICLE INFO

Article history:
Received 19 September 2014
Received in revised form
19 November 2014
Accepted 20 November 2014
Available online 26 November 2014

Keywords:
Environmental crazing
Polymer fibers
Nanoporous structure

ABSTRACT

Tensile drawing of glassy PET fibers via environmental crazing is studied. Direct microscopic observations show that this process includes the development of macroscopic porosity due to the initiation and growth of multiple crazes with their specific fibrillar-porous structure. Environmental crazing of fibers is characterized by the early collapse of the thermodynamically unstable structure of crazes. This process commences at the stage of craze widening and proceeds until the crazes lose their porosity and become fully monolithic. The collapse is provided by the coagulation of the flexible nanoscale craze fibrils via their interaction by side surfaces. The collapse is markedly intensified when the active liquid is removed from the volume of crazes and, as a result, the crazed fibers acquire a specific surface relief with alternating thick and thin regions corresponding to the bulk unoriented polymer and the collapsed crazes. Practical advantages of the stage of the collapse of the crazed nanoporous structure of crazes for the creation of the fiber-based nanocomposite materials are discussed.

1. Introduction

According to the general knowledge [1–7], crazing is the mode of the plastic deformation of solid polymers which is accompanied by the stress-induced development of the macroscopic porosity. When polymers are subjected to the action of the applied stress in the presence of an adsorptionally active liquid environment (AALE), their deformation proceeds via the development of numerous discrete zones of strain accommodation with their unique structural organization which are coined as crazes [1–3]. The inner structure of crazes consists of the oriented craze fibrils produced by the mechanism of the Taylor meniscus instability and the ends of fibrils are firmly fixed in the adjacent regions of the bulk polymer [6–8]. The typical diameter of the craze fibrils is equal to several nanometers (below 20 nm), and the spacing between the neighboring fibrils (pores or cavities) also lies within the nanometric scale [2,9,10]. However, the actual inner structure of crazes is far from the idealized case when fibrils are modeled as firm individual rods bridging the opposite craze walls but appears as a fibrillated weblike network [11]. Noteworthy is that the glass transition temperature of the polymer material in the nanoscale fibrils can be markedly depressed as compared with that of the bulk polymer [12,13], and this factor also contributes to structural organization and further evolution of the crazed material.

As compared with the deformation of solid polymers in air via the mechanism of crazing (so-called *dry crazing*) [1–3], tensile drawing of polymers in adsorptionally active liquid environments (*solvent crazing or environmental crazing*) is characterized by its own specific features provided by the action of a liquid environment on polymers [10,14–16]. In contrast to dry crazing, deformation via environmental crazing proceeds over a broad interval of tensile strains without fracture up to the stage of orientational strengthening, thus opening advantageous possibilities for the detailed study of this phenomenon and characterization of the structural evolution of the nanoporous fibrillated craze matter [15,17].

The process of environmental crazing (EC) includes several well-defined stages [10]. Fig. 1 shows the general scenario of environmental crazing of solid polymers in its comparison with the corresponding stress–strain diagram and the (porosity)-(tensile strain) curve.

At the early stages of stretching (at low tensile strains below the yield point), surface defects existing in the polymer sample give rise to the initiation of multiple crazes with their unique fibrillar-porous structure, which serve as the regions of strain accommodation (Fig. 1). The initiated crazes start to grow in the direction

* Corresponding author. Tel.: +7 495 9395509.
E-mail addresses: arzhakova8888@gmail.com (O.V. Arzhakova), dolgova2003@mail.ru (A.A. Dolgova), yarishev@gmail.com (L.M. Yarysheva), volynskii@mail.ru (A.L. Volynskii), NBakeev@gmail.com (N.F. Bakeev).

http://dx.doi.org/10.1016/j.polymer.2014.11.044
0032-3861/

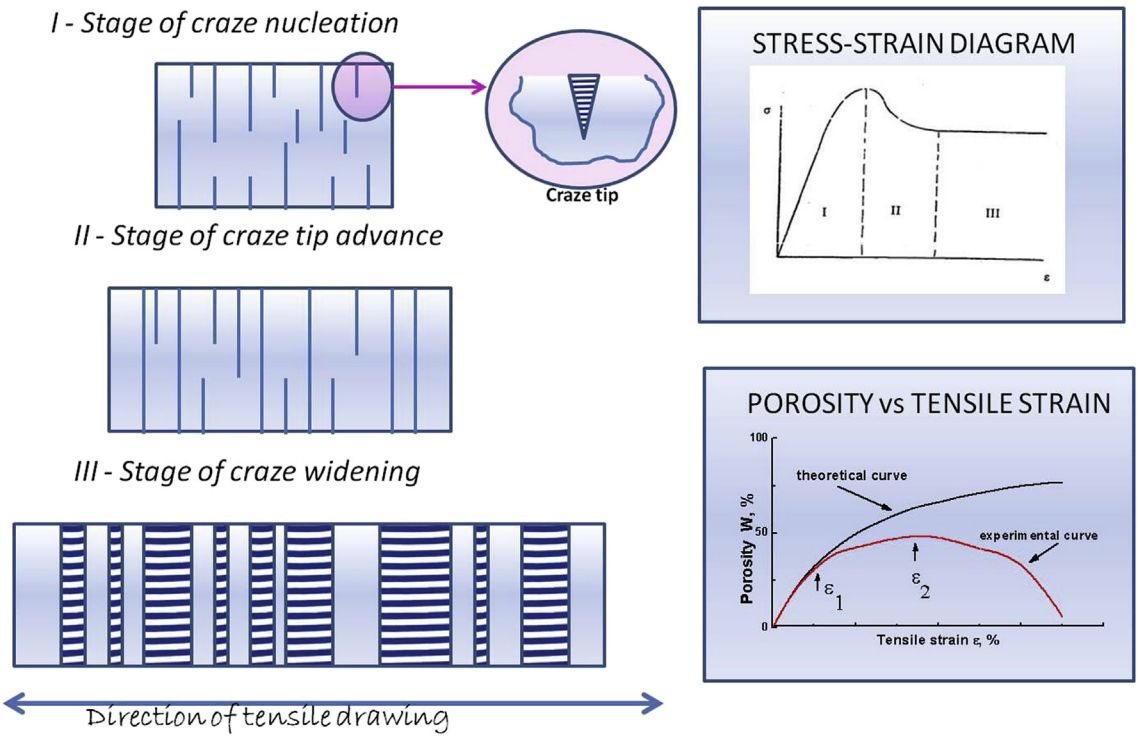

Fig. 1. Schematic representation of different stages of environmental crazing: I – the region of craze initiation, II – the region of craze tip advance, III – the region of craze widening or thickening. Correlation of the EC stages with the corresponding stress–strain diagram and (porosity)-(tensile strain) curve.

perpendicular to the direction of the applied stress (the stage of craze tip advance) [18,19]. At this stage, the width of crazes is low (several fractions of microns) and remains virtually unchanged. New crazes are initiated [20,21] until one or several initiated crazes at the stage of craze tip advance propagate through the whole cross section of the sample, and stress relaxation takes place (the yield tooth). Evidently, this process is strongly controlled by the geometry of the polymer sample, in particular, by its thickness. For example, as was shown in Ref. [22], the duration of this stage is naturally longer for thicker samples because the time required for crazes to pass the cross section of the sample is naturally longer. As a result, the density of the initiated crazes increases.

Once the initiated crazes pass through the whole cross section of the sample, the stage of craze widening or craze thickening comes into play when the growing crazes increase their width along the direction of tensile drawing and the craze walls are drifted apart. Naturally, this is the stage when most of the initial bulk polymer is transformed into the oriented state within the craze fibrils. The macroscopic porosity W of the sample increases with increasing ε according to the following law as $W = (\varepsilon/(\varepsilon + 1)) \times 100\%$ (the theoretical curve in Fig. 1) where W is the volume of the crazed regions per the overall volume of the sample, and ε is the tensile strain. The development of the marked macroscopic porosity with increasing tensile strain is possible only when the volume of nanoporous crazes is continuously filled up with the surrounding adsorptionally active liquid. It is important to mention that, according to the abundant experimental data collected by diverse physicochemical methods (X-ray analysis, TEM, pressure driven liquid permeability, etc.) [3,8,23], the diameter of the craze fibrils and the distance between the neighboring fibrils are of the same order and lie within the range of ~1–20 nm. The length of the craze fibrils is obviously equal to the distance between the craze walls. Thus, the craze fibrils can be treated as specific asymmetric colloidal particles with the fixed ends, and the whole craze can be compared to a specific colloidal system with a high level of surface energy.

The final stage of environmental crazing is concerned with the collapse of the nanoporous structure of crazes which takes place at high tensile strains when most of the polymer appears to be transformed into the oriented fibrillated state within crazes [10]. The onset of this stage can be detected from the deviation of the experimental W–ε curve from the theoretical dependence (ε_1 in the experimental W–ε plot in Fig. 1). This phenomenon can be explained as follows: the collapse of the nanoporous craze structure commences when, with increasing ε, the craze walls are drifted apart by a relatively long distance so that the fibrillar aggregates bridging the opposite craze walls become relatively long. As the length of the craze fibrils increases, they acquire a sufficient flexibility and the neighboring fibrils can contact each other by their lateral surfaces. This contact of the neighboring fibrils leads to their coagulation which provides so-called collapse of the nanoporous structure of crazes. Evidently, at this stage, the liquid entrapped within the nanoporous crazes is squeezed out or expelled from the sample (syneresis). Finally, the W–ε plot passes the maximum at a certain tensile strain (depicted as ε_2 in Fig. 1) and starts to decrease. Our earlier studies on the EC phenomenon for polymer films show that this stage of environmental crazing is strongly controlled by the geometry of the sample, in particular, by the thickness. For thicker films, the onset of the collapse and the maximum in W–ε plot are observed at much higher tensile strains: for example, $\varepsilon_1 = 75\%$ and $\varepsilon_2 = 175\%$ for the films with a thickness of 50 μm, and $\varepsilon_1 = 220\%$ and $\varepsilon_2 = 280\%$ for the films with a thickness of 300 μm [22]. Hence, for all stages of environmental crazing, the geometry of the sample is proved to be the critical factor that should be necessarily taken into account.

In this connection, of special interest is the study of environmental crazing for polymeric fibers as the samples with an alternative (critically different from the films) geometry. However, so

far, nearly all works on the mechanism of crazing (both dry crazing and environmental crazing) were performed for polymer films [1–7] whereas crazing of polymeric fibers virtually remains *terra incognita* even though few publications of the applied character [24–28] and several patents related to this subject [29–33] were available.

The objective of this work is concerned with the detailed study of the environmental crazing of polymeric fibers based on glassy PET and their structural evolution as well as with the description of the practical advantages of this phenomenon for the development of diverse fiber-based nanocomposite materials.

2. Materials and methods

In this work, we studied commercial unoriented fibers based on glassy amorphous PET as a thread composed of 25–30 filaments with a diameter of 35–38 μm. According to the DSC data, glass transition temperature of the PET fibers is 79 °C and, at ambient temperature, this polymer exists in the glassy state [34].

As an adsorptionally active liquid environment (AALE) promoting environmental crazing of PET, we used *n*-butanol (normal aliphatic alcohol). At room temperature, PET does not swell in this AALE.

Continuous stretching of polymeric fibers was performed using the modified labscale setup based on the standard DACA *Instruments* equipment. This stretching machine for tensile drawing of fibers in the continuous regime consists of a feed roller, two guide rollers, two rollers rotating at different rates, and a winding roll for collecting fibers after stretching. To provide environmental crazing and to stretch polymer fibers, a bath (15 ml) with an AALE (*n*-butanol) was placed in between the stretching rolls and stretching should be performed in the direct contact with an AALE. Continuous stretching of fibers was performed at a constant rate of 1 m/min at room temperature. Tensile strain was varied from 25% to 450%. All fibers studied in this work were prepared under the continuous mode unless otherwise specified.

For direct microscopic observations, tensile drawing of the PET fibers (the gauge length was 30 mm) in the AALE (*n*-butanol) was performed using hand-operating clamps in the batch regime. The tensile strain rate was 5 mm/min.

The development of the porous structure of the solvent-crazed fibers was studied using the technique of dye contrasting. As a contrasting dye, we used Rhodamine Blue (1.7 nm). The dye was dissolved in the AALE (*n*-butanol) and its saturated solution was prepared (10^{-4} g/L). Later, this alcohol dye-containing solution was used as the AALE for stretching under the continuous regime or under the batch mode or it was used in the sorption experiments when after stretching the solvent-crazed fibers were immersed in this dye-containing solution and allowed to stay for 24 h at room temperature.

Structure of the solvent-crazed fibers was studied using the method of light microscopy on a METAM polarization microscope (LOMO, Russian Federation) and an OPTON polarization microscope (Carl Zeiss, Germany) in the transmission mode as well as by the scanning electron microscopy on a Hitachi S-520 scanning electron microscope (Japan). For SEM studies, the samples were decorated with a thin conducting platinum layer.

The images of the solvent-crazed fibers were analyzed using the FemtoScan software (Advanced Technologies Center, Russian Federation).

3. Results and discussion

Let us consider the general scenario how the polymer fibers based on glassy PET are stretched in the AALE. First, visual observations over this process show that, after stretching in the AALE, initially transparent PET fibers become milky white thus attesting the development of multiple surface light-scattering imperfections with dimensions corresponding to the incident light wavelength. Reference experiments show that the cold drawing of the same PET fibers in air under the same conditions proceeds via necking and the stretched fibers remain transparent but become much thinner.

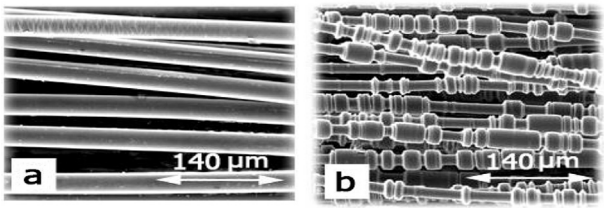

Fig. 2. SEM images of the initial PET fibers: initial fibers (a) and crazed PET fibers with a tensile strain of 100% (b).

Fig. 2 shows the SEM micrographs of the initial PET fibers (Fig. 2a) and crazed PET fibers after tensile drawing in *n*-butanol by 100% (Fig. 2b).

As follows from Fig. 2, the visual appearance of the environmentally crazed fibers appears to be amazingly different (Fig. 2b) from the initial fibers (Fig. 2a). The crazed fibers acquire a specific surface relief which is organized as alternating regions with different diameters (thick and thin regions), and the length of the alternating regions is equal to several microns or tens of microns. The evident difference from the PET fibers stretched in air via necking is that, upon necking, the sample narrows down at one site (which is a neck) (Fig. 3) whereas the solvent-crazed fibers seemingly contain multiple necks (Fig. 2b).

The development of this unique thin-and-thick relief was first described in the patents by Adams who naturally coined the observed thin regions as micronecks due to their visual similarity to necks [30,31]. A neck in polymers is known to be monolithic and contains no pores but crazes are naturally expected to be porous. Traditionally, the presence of the porous structure in polymers can be detected by the dye-contrasting experiments which, in our work, were performed in the following manner: the crazed fibers after stretching in AALE and the fibers stretched in air via necking were placed into the dye-containing solution for 48 h at room temperature, and it was found that both fibers remain virtually uncolored. This fact conveys that the fibers contain no porous structure and the thin regions along the crazed fibers are truly monolithic and can be treated as micronecks. However, when the same fibers are stretched in the dye-contrasting solution of AALE, the crazed fibers are seen to be brightly colored. The microscopic images show that the fibers are colored not throughout their full length but only thin regions became colored whereas the thick regions remain uncolored (Fig. 4). Hence, one may conclude that stretching of the PET fibers in the AALE is accompanied by the development of the porous structure via crazing and by the active

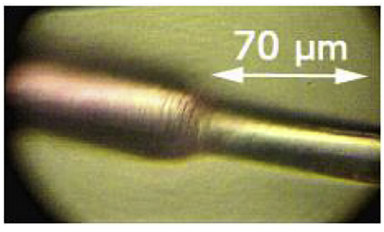

Fig. 3. The PET fiber after stretching in air via necking.

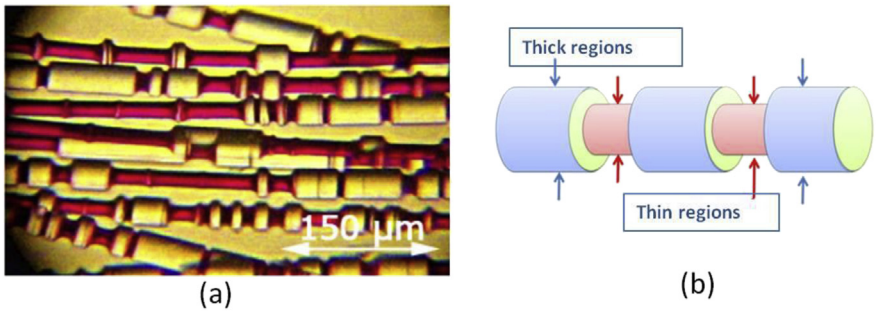

Fig. 4. (a) Optical micrographs of the solvent-crazed PET fibers after their tensile drawing in the dye-containing AALE by 150% (a) and (b) their schematic idealized representation.

penetration of the dye molecules into the crazed structure but later, by some reason, the colored regions become fully monolithic.

Let us now consider the structural evolution taking place in the PET fibers upon their tensile drawing in AALE with increasing tensile strain. Fig. 5 shows the SEM images of the solvent-crazed PET fibers as the tensile strain increases from 50 to 350%. The presented SEM images vividly illustrate that, with increasing tensile strain, the fibers experience dramatic structural changes.

As follows from the SEM images in Fig. 5, as the tensile strain ε increases, the entire macroscopic elongation of the sample is provided solely via the increase in the length of the thin regions but the overall (summed) length of the thick regions decreases. The thin regions can be attributed to the formed crazes whereas the thick regions correspond to the initial undeformed polymer, and their diameter fully coincides with the diameter of the initial unoriented fibers.

As the tensile strain increases, the fractional content of unoriented thick regions decreases (from 100% down to 0%) whereas the fraction of the thin regions increases (from 0 to 100%) (Fig. 5). As follows from Fig. 5f and g, the PET fibers stretched by $\varepsilon = 250\%$ still contain very short thick regions but their fraction is low. As the tensile increases up to $\varepsilon = 300\%$, all thick regions disappear, and the resultant fibers become smooth and optically transparent. By their visual appearance, the fibers stretched by 300% are virtually similar to the fibers stretched in air via necking. Hence, one can conclude that the transformation of the polymer into the fully oriented state is finished at the draw ratio of 3.8–4.0, which corresponds to the natural draw ratio of PET [6].

Examination of the SEM images of the solvent-crazed PET fibers over the entire interval of tensile strains makes it possible to observe that, independently of the macroscopic tensile strain ε, the diameter of thick cylindrical regions is constant and equal to the diameter of the initial unoriented fibers. Another remark concerns the fact that the diameter of the thin regions is also invariable and is also independent of the macroscopic tensile strain ε in the entire region of tensile strains (Fig. 5).

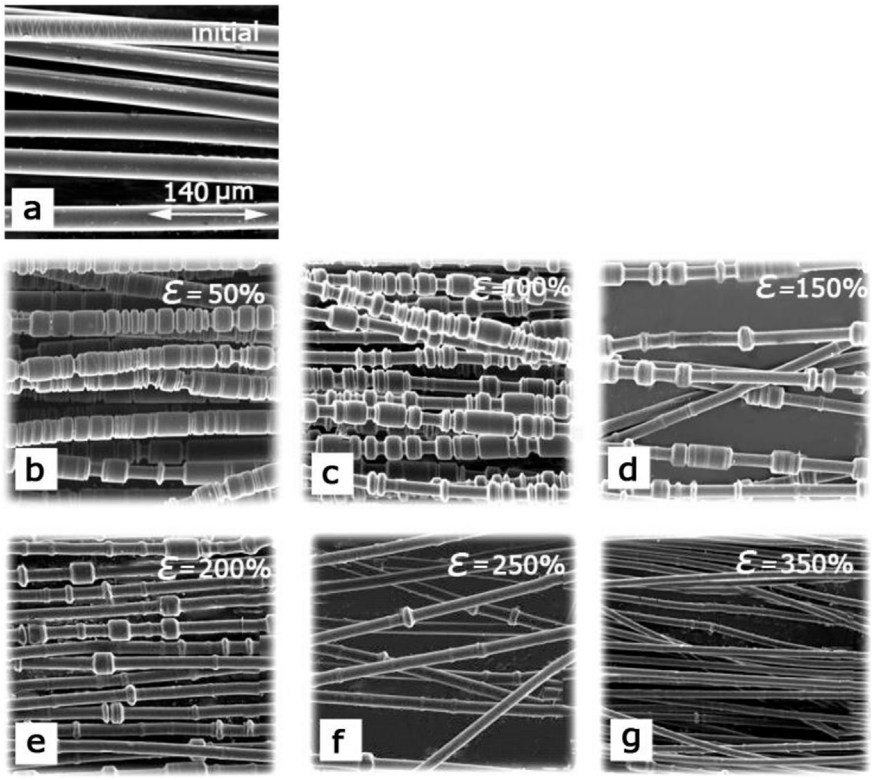

Fig. 5. The SEM images of the PET fibers: (a) initial unoriented PET fibers and PET fibers after their tensile drawing in AALE by a tensile strain of (b) 50, (c) 100, (d) 150, (e) 200, (f) 250, and (g) 350%.

From the presented SEM images (Fig. 5), the diameters of thick and thin regions of the solvent-crazed fibers are estimated to be equal to (40 ± 3) and (20 ± 2) microns, respectively. According to the geometric formula, the volume of a cylinder reads as $V = \pi R^2 h$, where R is the diameter and h is the height of the cylinder. Thus, for polymeric fibers, R is the radius of the fibers, and h is its length. Therefore, assuming that deformation proceeds via the development of a monolithic neck from the cylindrical initial unoriented fiber with the radius R (or diameter $2R$) and length h, a new cylinder with the radius r and length $h\lambda$ is formed where λ is the natural draw ratio (NDR) of the polymer: $\pi R^2 h = \pi r^2 \lambda h$. Hence, the natural draw ratio λ can be calculated as the ratio between the volumes of the initial and necked parts of the fiber (Fig. 4 b) as $\lambda = R^2/r^2$.

In the case of the crazed PET fibers, this ratio for thick and thin regions is equal to 3.8–4.0. This value fully corresponds to the NDR of PET as estimated by independent studies [6]. This correspondence conveys that the thin fragments in the crazed fibers are fully monolithic and do not contain any pores, or in other words, their structure is similar to the structure of the polymer in the neck.

Invariable diameter of the thin regions corresponding to crazes also directly proves the mechanism of the surface drawing of the polymer material upon crazing, and this conclusion agrees with the results of the earlier studies on the environmental crazing of the PET films upon their tensile drawing in the AALE obtained by different methods such as X-ray analysis, pressure-driven liquid permeability, and DSC [3,10,23].

The question arises when and how the initial porous structure of crazes becomes monolithic. To answer this question, we studied deformation of the PET fibers in the AALE by direct microscopic on-line observations. The fibers were fixed in the hand-operating clamps and enveloped by transparent plastic bags filled with the AALE (n-butanol), and thus coated sample was placed onto a microscope stage. The collected digital images are presented in Fig. 6.

As follows from the presented snapshots, deformation of the PET fibers in the AALE proceeds via the initiation of well-pronounced crazes which are seen as more transparent regions. With increasing macroscopic tensile strain ε to 150%, the craze walls are seen to be drifted apart (the stage of craze widening) but

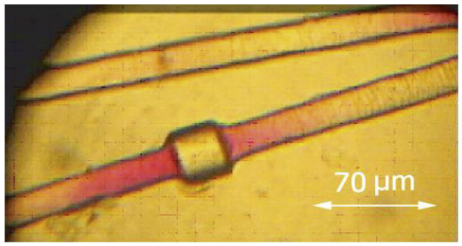

Fig. 7. The optical micrographs of the PET fibers after the tensile drawing in the AALE by 150% and staying in the dye-containing solution (Rhodamine B in n-butanol) for 24 h.

the structure of the stretched fibers is different from that shown in Fig. 5: there is no decrease in the diameter of the fibers in the crazed regions, and the fibers do not have any surface relief (Fig. 6a–c).

These on-line microscopic observations make it possible to visualize the development of the macroscopic porosity in the PET fibers. The porosity W (the volume of the crazed regions) is seen to increase with increasing ε as $W = \varepsilon/\varepsilon + 1 \times 100\%$. Now, it seems clear why and how the dye molecules (or any additives dissolved in the AALE) are able to penetrate the PET fibers upon their tensile drawing in the AALE.

However, as follows from Fig. 6, as the tensile strain ε is higher than 150%, one can observe that the central part of the crazed regions becomes thinner, and this thinning becomes even more pronounced with increasing tensile strain (or craze width). Now we can expect that when this decrease in the diameter of the crazed regions achieves the thickness of the air-drawn neck (for the fibers after their stretching in air via necking), the collapse of the porous structure is completed, and the crazes lose their porosity and become monolithic.

To prove this assumption, the following experiments were carried out. The stretched fibers immediately after their tensile drawing in the AALE (wet fibers) were immersed into the dye-containing solution of AALE (the solution of Rhodamine Blue in

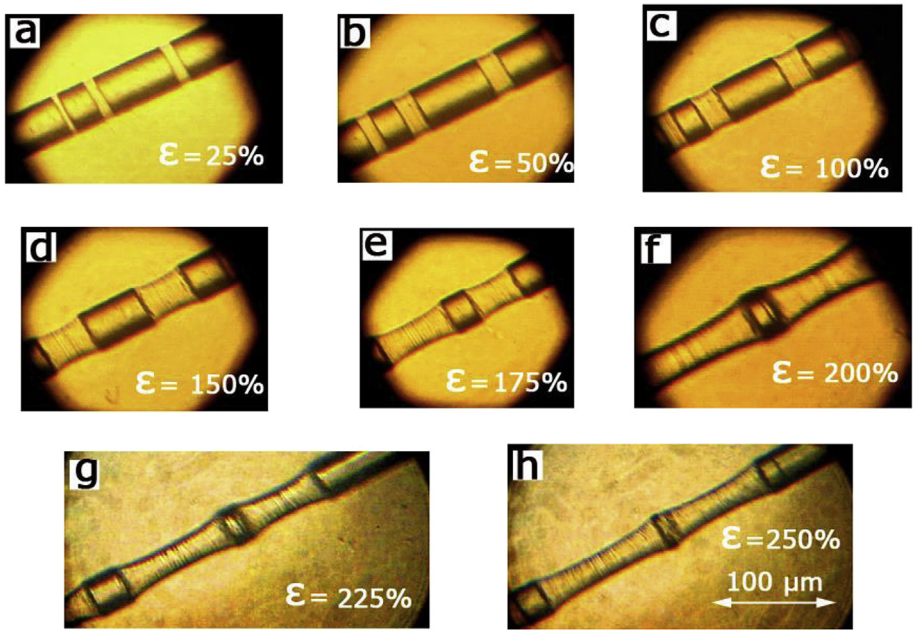

Fig. 6. The micrographs of the PET fibers upon their tensile drawing in the AALE (n-butanol) in the regime of on-line microscopic observations.

n-butanol) and allowed to stay there for 24 h. The snapshots of these fibers are shown in Fig. 7.

As follows from Fig. 7, the fibers are colored only in the regions adjacent to the craze walls but their thinned central part is colorless. This evidence allows one to conclude that the regions near the craze walls preserve their porosity thus allowing penetration of the dye molecules into their structure via diffusion. The fact that the central regions of crazes stay uncolored means that the dye molecules are unable to penetrate their structure, thus proving that the initially formed porous structure is collapsed and becomes monolithic. Hence, the collapse of the porous structure of crazes commences in the course of the tensile drawing in the AALE and progresses with increasing tensile strain (as crazes become wider). Finally, at high tensile strains (above NDR), the solvent-crazed fibers become fully monolithic and can be compared to the fibers stretched in air via necking (see Fig. 5g).

In whole, the collapse of the porous structure of crazes can be briefly explained as follows. According to the general knowledge, the inner structure of crazes is composed of the interconnected craze fibrils whose length corresponds to the craze width and their diameter lies within the nanoscale interval [1,4]. Thus, the fibrils can be treated as the specific colloidal asymmetric particles whose ends are firmly fixed at the craze walls, and each single craze is a closed colloidal system with a highly developed surface and with a high level of excessive surface energy. This colloidal system is thermodynamically unstable and tends to reduce its high surface energy by reducing its specific surface. This can be achieved by the coagulation of craze fibrils. However, the coagulation of the craze fibrils is hindered because the fibrils are fixed at the craze walls and can be compared to a stretched string. As the craze width increases, the fibrils increase their length along the direction of tensile drawing and acquire mobility in the lateral direction. This lateral motion allows them to interact by their side surfaces and coagulate first through the pointlike contacts and later by longer regions. The maximum amplitude of the lateral motions of the craze fibrils is achieved at the central part of the craze and, hence, their interaction becomes more intensive, thus giving rise to the coagulation. Due to the coagulation, excessive free energy of the nanoporous structure is reduced and the overall porosity decreases. Finally, when the tensile strain approaches the NDR, this leads to the complete healing of porosity and the fibers become monolithic like the fibers drawn in air via necking.

However, even at moderate tensile strains well below the NDR, when the AALE is removed from the solvent-crazed samples by drying, the collapse of the porous structure within the crazes is intensified: as a result, the porosity within each craze is healed, and the crazes are gradually degenerated into monolithic micronecks. The result of this local collapse is the development of a unique surface relief which is composed of alternating thin (former crazes) and thick regions (unoriented bulk polymer) as shown in Fig. 5. As the proof of the complete monolithization, the diameter of the thin regions fully corresponds to the diameter of the air-necked fibers.

Noteworthy is that it is the collapse of the fibrillated porous structure of crazes that serves as the prerequisite for the multistage coloring of the polymer fibers described in the patent by Adams [31]. This multistage coloring can be accomplished only when, after stretching of the polymer fibers in the dye-containing solution via crazing, the conditions providing the complete collapse and transformation of crazes into monolithic micronecks are achieved. But the necessary condition is that the fibers should still contain sufficient amounts of uncrazed regions. As a result of the subsequent stretching of these fibers in a solution containing a differently colored dye, new crazes are initiated and their newly formed porous structure is filled with the dye-containing solution but the collapsed monolithic regions corresponding to the former crazes from the first coloring cycle remain closed and impermeable for the new portions of the AALE. The results of our experiments with multistage coloring are shown in Fig. 8. These coloring cycles can be repeated several times with different dyes, provided the fibers still contain sufficient amounts of the bulk unoriented polymer regions where new crazes can be initiated.

As a result, the controlled collapse upon the environmental crazing allows preparation of the multicolored fibers containing differently colored regions with micronic dimensions and, to our best knowledge, this pattern cannot be achieved by any other method. Naturally, this approach based on the environmental crazing offers broad possibilities for the introduction of not only dyes but also diverse incompatible low-molecular-mass additives thus providing the unique opportunity for the preparation of various multicomponent nanocomposite fiber-based materials with unique characteristics related to the functionalities of the introduced additives.

4. Conclusions

For the first time structural evolution of polymer fibers based on glassy PET upon environmental crazing was studied. Direct on-line microscopic observations show that tensile drawing of PET fibers in the AALE proceeds via the mechanism of crazing which includes the development of the macroscopic porosity due to the initiation and growth of multiple crazes with their specific fibrillar-porous structure. The experimental data reveal that the distinctive feature of environmental crazing of polymer fibers is concerned with the early collapse of the thermodynamically unstable nanoporous structure of crazes which provides a gradual reduction in the porosity of the crazed fibers down to their complete monolithization. The collapse of the crazed fibrillated porous structure commences at the stage of craze thickening (craze widening) in the course of the tensile drawing of the fibers in the AALE. This process is provided by the coagulation of the craze fibrils which acquire the sufficient mobility allowing their interaction with the neighboring fibrils by lateral surfaces. This interaction between the neighboring craze fibrils becomes more intensive with increasing tensile strain as the crazes increase their width, thus finally leading to the formation of fully monolithic and oriented fibers which are similar to the fibers stretched in air via necking. The complete collapse of the nanoporous structure can be also achieved at moderate tensile strains when the AALE is removed from the crazes by drying: the porous crazes lose their porosity and become monolithic, thus forming so-called micronecks and the crazed fibers acquire a specific surface relief with alternating thin (former crazes or micronecks) and thick regions (unoriented bulk polymer). Some practical advantages of the controlled collapse upon the environmental crazing for the preparation of diverse nanocomposite fiber-based materials are highlighted.

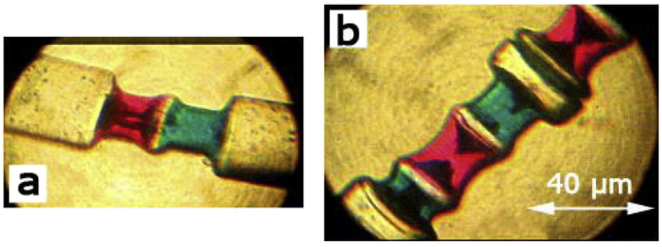

Fig. 8. The crazed PET fibers after the multistage coloring cycles via environmental crazing: (stage 1) stretching by 75% in AALE (*n*-butanol) containing dissolved Rhodamine B and drying and (stage 2) stretching by 75% in AALE (*n*-butanol) containing dissolved Brilliant Green and drying. (For interpretation of the references to colour in this figure legend, the reader is referred to the web version of this article.)

Acknowledgments

The reported study was partially supported by RFBR, research project no. 14-03-00617_a and by the Grant for the State Support of Leading Scientific Schools, NSh-1683.2014.3.

References

[1] Kambour RP. A review of crazing and fracture in thermoplastics. J Polym Sci Macromol Rev 1973;7:1–56.
[2] Kramer EJ. Microscopic and molecular fundamentals of crazing. In: Kausch HH, editor. Crazing in polymers, Adv in Polym Sci, vols. 52/53. Springer Berlin Heidelberg; 1983. p. 1–56. http://dx.doi.org/10.1007/BFb0024055.
[3] Kausch HH, editor. Crazing in polymers vol. 2. Adv polymer Sci, vols. 91/92. Springer Berlin Heidelberg; 1990, ISBN 978-3-540-51306-3.
[4] Donald AM. Crazing. In: Haward RN, Young RJ, editors. The physics of glassy polymers. 2nd ed. London-N.Y: Chapman & Hall; 1997, ISBN 0-412-62460-5. p. 295–342.
[5] Estevez R, Tijssens MGA, Van der Giessen E. Modeling of the competition between shear yielding and crazing in glassy polymers. J Mech Phys Solids 2000;48:2585–617. http://dx.doi.org/10.1016/S0022-5096(00)00016-8.
[6] Ward IM, Sweeney J. An introduction to the mechanical properties of solid polymers. 2nd ed. England: John Wiley & Sons; 2004, ISBN 978-0-471-49626-7.
[7] Argon AS. Craze initiation in glassy polymers-revisited. Polymer 2011;52:2319–27. http://dx.doi.org/10.1016/j.polymer.2011.03.019.
[8] Kramer EJ. Craze fibril formation and breakdown. Polym Eng Sci 1984;24:761–9. http://dx.doi.org/10.1002/pen.760241006.
[9] Michler GH. Electron microscopy of polymers. Springer Berlin Heidelberg; 2008, ISBN 978-3-540-36352-1.
[10] Volynskii AL, Bakeev NF. Solvent crazing of polymers. Amsterdam: Elsevier; 1995, ISBN 0-444-81848-0.
[11] Donald AM, Kramer EJ. The entanglement network and craze micromechanics in glassy polymers. J Polym Sci Polym Phys Ed 1982;20:1129–41. http://dx.doi.org/10.1002/pol.1982.180200703.
[12] Keddie JL, Johnes RAL, Cory RA. Size-dependent depression of the glass transition temperature in polymer films. Europhys Lett 1984;27:59–64. http://dx.doi.org/10.1209/0295-5075/27/1/011.
[13] Boucher VM, Cangialosi D, Yin H, Schonhals A, Alegrıa A, Colmenero J. T_g depression and invariant segmental dynamics in polystyrene thin films. Soft Matter 2012;8:5119–22. http://dx.doi.org/10.1039/C2SM25419K.
[14] Brown HR, Kramer EJ. Effect of surface tension on the stress in environmental crazes. Polymer 1981;22:687–90. http://dx.doi.org/10.1016/0032-3861(81)90362–1.
[15] Brown HR. A model of environmental craze growth in polymers. J Polym Sci Part B Polym Phys 1989;27:1273–88. http://dx.doi.org/10.1002/polb.1989.090270607.
[16] Yaffe MB, Kramer EJ. Plasticization effects on environmental craze microstructure. J Mater Sci 1981;16:2130–6. http://dx.doi.org/10.1007/BF00542373.
[17] Yang AGM, Kramer EJ. Craze fibril structure and coalescence by low-angle electron diffraction. J Polym Sci Polym Phys Ed 1985;23:1353–67. http://dx.doi.org/10.1002/pol.1985.180230705.
[18] Bucknall CB. New criterion for craze initiation. Polymer 2007;48:1030–41. http://dx.doi.org/10.1016/j.polymer.2006.12.033.
[19] Basua S, Mahajana DK, Van der Giessen E. Micromechanics of the growth of a craze fibril in glassy polymers. Polymer 2005;46:7504–18. http://dx.doi.org/10.1016/j.polymer.2005.05.148.
[20] Rottler J, Robbins MO. Growth, microstructure and failure of crazes in glassy polymers. Phys Rev E 2003;68. http://dx.doi.org/10.1103/PhysRevE.68.011801. 011801-1–011801-18.
[21] Marissen R. Craze growth mechanics. Polymer 2000;41:1119–29. http://dx.doi.org/10.1016/S0032-3861(99)00234-7.
[22] Volynskii AL, Arzhakova OV, Yarysheva LM, Bakeev NF. Features of deformation of polyethylene terephthalate films of various thicknesses in adsorption active media. In: Russian, title © 2014 Thomson Reuters Vysokomolekulyarnye Soedineniya Seriya A, vol. 31; 1989. p. 2673–7.
[23] Yarysheva LM, Gal'perina NB, Arzhakova OV, Volynskii AL, Bakeev NF, Kozlov PV. Using of the liquid permeation method to determine the structure of crazes arising under deformation of polymers in liquid media. In: Russian, title © 2014 Thomson Reuters Vysokomolekulyarniya Soedineniya Seriya B, vol. 31; 1989. p. 211–6.
[24] Weichold O, Goel P, Lehmann KH, Möller M. Solvent-crazed PET fibers imparting antibacterial activity by release of Zn2+. J Appl Polym Sci 2009;112:2634–40. http://dx.doi.org/10.1002/app.29818.
[25] Sokkar TZN, El-Farahaty KA, Azzam AAS. On-line interferometric study on the mechanical fracture behaviour by crazing observed in stretched polypropylene fibres. Fibers Polym 2014;15:605–13. http://dx.doi.org/10.1007/s12221-014-0605-1.
[26] Pinchuk LS, Gol'dade VA, Kuz'menkova NV, Sytsko VE, Lobanovskii LS, Drozd ES. Modification of polyester fibers for protection of securities. Fibre Chem 2013;44:273–9. http://dx.doi.org/10.1007/s10692-013-9445-9.
[27] Gol'dade VA, Pinchuk LS, Vinidiktova NS. Modification of polyester fibers by bactericides using crazing mechanism. Int Polym Process 2010;25:199–204. http://dx.doi.org/10.3139/217.2321.
[28] Andronova AP, Popryadukhina SI, Egorov IA, Aleshicheva NB. Dyeing polyester fibers using the crazing method. Fibre Chem 2011;43:86–9. http://dx.doi.org/10.1007/s10692-011-9312-5.
[29] Sheljakov OV, Ivanov MN, Volynskij AL, Bakeev NF, Yarysheva LM, Arzhakova OV, et al. N.I. Nikonorova RUS Patent 2394948; 2010.
[30] Adams D. US Patent 3,102,323; 1963.
[31] Adams D. US Pat 3,233,019; 1966.
[32] Bakeev NF, Lukovkin GM, Marcus I, Mikushev AE, Shitov NA, Vanissum BE. A.L. Volynskii US Patent 5,516,473; 1996.
[33] Volynskii AL, Bakeev NF, Yarysheva LM, Dolgova AA, Arzhakova OV, Rukhlja EG, et al. A.V. Olenin RUS Patent 237056; 2009.
[34] Brandrup J, Immergut EH, Grulke EA, Abe A, Bloch DR, editors. Polymer handbook. 4th ed. NY: Wiley-Interscience Publication, John Wiley & Sons, Inc; 1999, ISBN 0-471-16628-6.